ON THE ABUNDANCE OF MULTISTABILITY IN THE HÉNON MAP

Paulo Cesar Rech[a,b], Marcus Werner Beims[b] and Jason A.C. Gallas[a,c,d]

[a]Departamento de Física, Universidade do Estado de Santa Catarina,
89223-100 Joinville, Brazil
[b]Departamento de Física, Universidade Federal do Paraná,
81531-990 Curitiba, Brazil
[c]Instituto de Física, Universidade Federal do Rio Grande do Sul,
91501-970 Porto Alegre, Brazil
[d]Institut für Computer Anwendungen, Universität Stuttgart,
D-70569 Stuttgart, Germany
e-mail: jgallas@if.ufrgs.br
WWW: http://www.if.ufrgs.br/∼jgallas

Abstract—*We report results of a systematic investigation concerning the relative abundance of multistability in the parameter space of the Hénon map. We also investigate how the relative volume of basins of attraction evolve when parameters are changed. In particular, we describe the variation along the familiar* $0 \to 1$ *line where saddle-node bifurcations occur, the* $1 \to 2$, $2 \to 4$, $4 \to 8$ *and* $8 \to 16$ *bifurcation lines as well as the path along which one may recover the dissipation rate from metric properties of self-similar structures in phase-space.*

The investigation of coupled oscillator systems is a topic of active research since such oscillators are known to describe phenomena as diverse as coupled p-n junctions[1], Josephson-junction arrays[2], phase synchronization of chaotic systems[3], bifurcations and global stability of synchronized states[4], high-Q cavity-induced synchronization in oscillator arrays[5] and much more[6].

The goal of this paper is to report an investigation of certain metric properties of a prototypical dissipative system, the Hénon map

$$x_{t+1} = a - x_t^2 + by_t, \qquad y_{t+1} = x_t.$$

We wish to assess two basic properties: (i) to quantify the relative abundance of multistability and (ii) to measure how the relative volume of basins of attraction vary when parameters are changed.

Our motivation for asking these questions has two different origins: first, such answers are needed when one wishes to consider a more flexible and realistic map, like the Hénon oscillator here, as the unit ruling local dynamics on a lattice of coupled maps in practical applications such as, for example, to simulate aspects of ocean convection[7], [8]. Although both questions above are of an elementary nature, their answers are quite hard to obtain: in the absence of adequate theoretical means even to estimate the answers, one needs to resort to intensive direct computations, and this is what we have done. Our second motivation has to do with our effort to understand as much as feasible the arithmetical origin of all features routinely observed in the parameter space of dynamical systems[9], [10], [11], [12], [13], [14], [15], [16].

We start presenting results about the relative basin volume. We consider two special types of paths in parameter space: the lines forming the boundaries of stability domains and an additional path, an *eigenvalue path*[9], [10], which is interesting since on this path one may recover the dissipation by measuring the scaling of certain fractal fingers that appear in phase-space.

Figure (1) shows the loci defined by the roots of these curves near to the physically interesting domain $-1 \leq b \leq 1$. The loci corresponding to the $4 \to 8$ and $8 \to 16$ bifurcations lie near the curve labeled 4, to the right. The boundaries of period-1, period-2 and period-4 stability domains are the roots of $\mathbb{U}(a,b) = 0$, $\mathbb{D}(a,b) = 0$ and $\mathbb{Q}(a,b) = 0$, where,

$$\mathbb{U}(a,b) \equiv a + \frac{1}{2}(1-b)^2, \tag{1}$$

$$\mathbb{D}(a,b) \equiv a - \frac{3}{4}(b^2 - 2b + 1), \tag{2}$$

$$\mathbb{Q}(a,b) \equiv a - \frac{1}{4}(5b^2 - 6b + 5), \tag{3}$$

The eigenvalue path contains an upper and a lower branch, defined by $\mathbb{E}(a,b) = 0$, where[9]

$$\mathbb{E}(a,b) = 4\,a\,b^2 - (b^2+b+1)\,(b^2+3\,b+1)\,(b-1)^2.$$

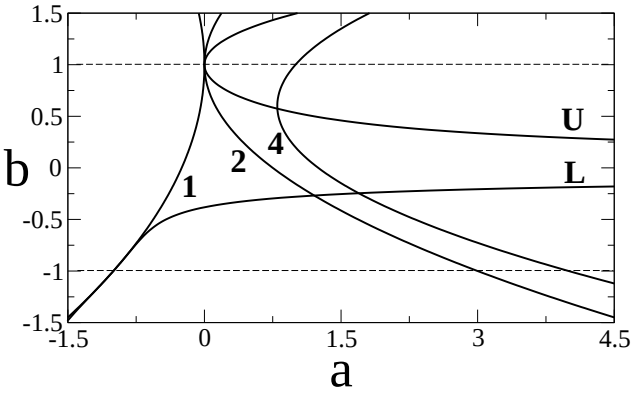

Fig. 1. Stability boundaries for low-period motions. Numbers label the curves where bifurcations occur: curve 1 marks the saddle-node $0 \rightarrow 1$ bifurcation, 2 marks the $1 \rightarrow 2$ bifurcation while 4 marks the $2 \rightarrow 4$ bifurcation. U and L refer to the upper and lower branches of the *eigenvalue path*, the path along which one may recover parameter values by measuring properties of fractal structures in phase space (see text).

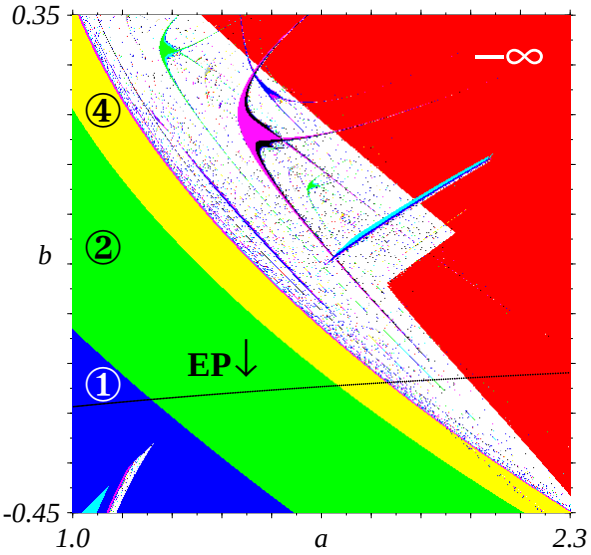

Fig. 2. Phase diagram showing the intricate alternation of stability domains underlying the lower branch of the eigenvalue path (indicated by EP). Different gray shadings represent stability domains of attractors with different periods. The encircled numbers denote the periodicity of the underlying domain. The white domain represents chaos. The basin of unbounded attractors is

Figure (2) shows the complexity of the alternation of the stability domains around the lower branch of the eigenvalue path, recognizable by the alternation of the gray shadings. The wide white domain lying roughly along the "main diagonal" of the figure indicates parameters for which *chaotic* solutions are stable. The different shadings (tonalities) embedded in the white domain represent domains os stability for *periodic* attractors, different shadings indicating different periodicity. The large gray domain seen on the upper right corner signals parameters leading mainly to unbounded solutions, i.e. to the attractor located at an infinite distance. The figure was generated using the method described in Ref. [16] where additional details may be found.

For each of the lines in Fig. (1), we considered 2000 points (a, b), from $-1 \leq b \leq 1$, and for each of them determined histograms of the periodicities as observed in phase-space, covering the window $-2.5 \leq x \leq 2.5$ and $-11 \leq y \leq 11$, discretized with a resolution of $100 \times 100 = 10^4$ points. This windows contains the largest portion of the 'useful' range of initial conditions, namely of those conditions not in the basin at infinity.

Figure (3) presents the fraction of the 10^4 initial conditions that do not diverge while moving from $b = -1$ to $b = 1$ along the saddle-node $0 \rightarrow 1$ line (indicated by 1), and the $1 \rightarrow 2$ and $2 \rightarrow 4$ bifurcation lines. Noteworthy is the fact that the volume increases with the unfolding of the bifurcation cascade. Furthermore, independently of the period, the volume

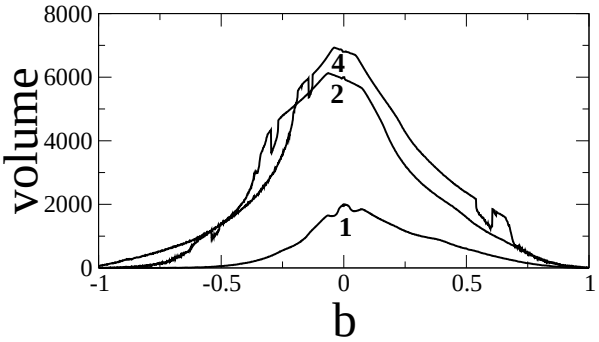

Fig. 3. Basin volume for the three lowest members of the 1×2^n cascade, as a function of the dissipation b.

tends to zero near $b = \pm 1$, the conservative (Hamiltonian) limit of the model, taking its maximum value for $b = 0$, the limit where the map is non-invertible (non-diffeomorphic). Figure (3) displays a few abrupt discontinuities, indicating domains where one finds multistability[17]. When all coexisting periods are added, no discontinuities exist. We checked these results using different discretizations and believe them to be accurate and representative.

Figure (4) gives the volume of period-16 motion and essentially reproduces what is found for period-4 and 8 (not shown here), indicating that the major change. While moving along the boundary between

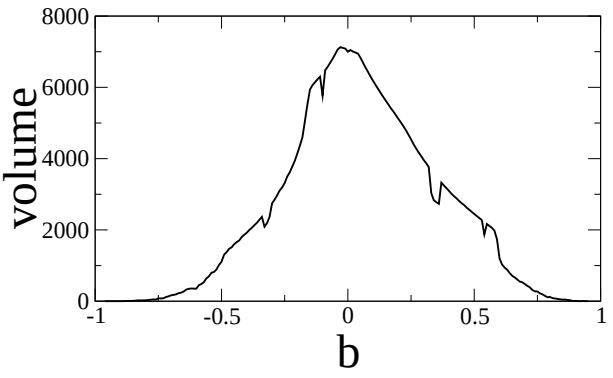

Fig. 4. Basin volume for period-16 attractors as a function of the dissipation b.

periods 8 and 16 one crosses several windows of periodicity, e.g. periods of the 3×2^n cascade, periods 96, 9, 18, 20, etc.

From a similar analysis, done while moving along the lower branch L of eigenvalue path $\mathbb{E}(a, b) = 0$, one discovers several features which, for reasons of space, cannot be addressed here. One result worth mentioning is that the basin size of the 3×2^n cascade during 6 bifurcations (up to period 96) remains essentially the same, reproducing the behavior observed for the 1×2^n cascade (see Fig. (4)). The basin of the coexisting period-2 motion remains also essentially constant. Moving along L up to $b = -0.26299$ one crosses a number of cascades, e.g. those starting with periods 9, 15, 21, 27, 33, 45, 63, 75, 105, windows separated by chaos. Moving beyond $b = -0.26299$ one finds the attractors as summarized in Table I where, to save space, a few small windows were omitted in some intervals.

Continuing to move along the L branch of the eigenvalue path, we now investigate what happens with the relative size of coexisting basins as the bifurcation process unfolds. For instance, given that at the boundary where periods 1 and 3 are born the respective size of their basin is 37% and 28%, which are relative sizes for periods 2 and 6, 4 and 12, etc? These numbers, shown in Table II, were obtained from the *average basin size* calculated for about 100 values ($\Delta b \simeq 10^{-5}$) in the (usually small) intervals of stability. Table III displays similar results for the 18×2^n cascade.

In conclusion, from the results above one sees that basin sizes remain essentially constant as the bifurcation unfolds. From the numbers obtained we have been also able to derive scaling laws for basin sizes and to quantify how basin sizes accumulate while converging toward a fixed size, among other things. As mentioned before, these results are quite robust upon changes of the discretizations involved in their derivation. These interesting metric properties will be presented elsewhere.

The authors thank CAPES and CNPq, Brazil, for support.

REFERENCES

[1] A. G. Mal'shukov and K. A. Chao, Phys. Rev. Lett. **86** (2001) 5570; R.V. Bursik and C. Jeffries, Phys. Rev. A, **31** (1985) 3332.

[2] B.C. Daniels, S.T.M. Dissanayake and B.R. Trees, Phys. Rev. E, **67** (2003) 036607. K. Wiesenfeld and P. Hadley, Phys. Rev. Lett., **62** (1989) 1335.

[3] K. Josic and D.J. Mair, Phys. Rev. E, **64** (2001) 056234.

[4] J. Acebrón, A. Perales and R. Spigler, Phys. Rev. E, **64** (2001) 016218.

[5] G. Filatrella, N.F. Pedersen and K. Wiesenfeld, Phys. Rev. E,]bf 61 (2000) 2513.

[6] See the review by: S. Boccaletti, J. Kurths, G. Osipov, D.L. Valladares and C.S. Zhou, Physics Reports, **366** (2002) 1-101.

[7] P. G. Lind, S. Titz, T. Kuhlbrodt, J. Corte-Real, J. Kurths, J. A. C. Gallas and U. Feudel, *Coupled bistable maps: a tool to study convection parameterization in ocean models*, Intern. J. Bif. Chaos, **13** (2003), in print.

[8] P. G. Lind, J. Corte-Real and J. A. C. Gallas, *Effects of local nonlinearity and basin size in the dynamics of lattices of bistable maps*, Proceedings of the Medyfinol, Colonia del Sacramento, Uruguay, December, 2002. Submitted to Physica A, 2003.

[9] P. C. Rech, M.W. Beims and J.A.C. Gallas, Europhys. Lett., **49** (2000) 702.

[10] P. C. Rech, M.W. Beims and J.A.C. Gallas, Physica A, **283** (2000) 273.

[11] A. Endler and J.A.C. Gallas, Phys. Rev. E, **65** (2002) 036231.

[12] J.A.C. Gallas, Phys. Rev. E, **63** (2001) 016216.

[13] B. Hunt, J.A.C. Gallas, C. Grebogi, J.A. Yorke and H. Koçak, Physica D, **129** (1999) 35.

[14] J.A.C. Gallas, Appl. Phys. B, **60** (1995) S-203. Festschrift Herbert Walther, special supplement.

[15] J.A.C. Gallas, C. Grebogi and J.A. Yorke, Phys. Rev. Lett., **71** (1993) 1359.

[16] J.A.C. Gallas, Phys. Rev. Lett., **70**, (1993) 2714.

[17] F. T. Arecchi, R. Meucci, G. Puccioni and J. Tredicce, *Phys. Rev. Lett.*, **49** (1982) 1217.

Attractor(s)	b interval	a interval	%
$2, 4, ..., 64, -\infty$	[-0.26298,-0.24060]	[1.30261324,1.82574913]	–
$-\infty$	[-0.24059,-0.24012]	[1.8260199,1.83878849]	65
$12, 24, -\infty$	[-0.24011,-0.24007]	[1.83906106,1.84015174]	34, 65
$144, -\infty$	-0.24006	1.8404245	12, 65
$36, -\infty$	-0.24005	1.84069731	34.5, 65.5
$-\infty$	[-0.24004,-0.23978]	[1.84097015,1.84807727]	65
$6, 12, ..., 48, -\infty$	[-0.23977,-0.23946]	[1.84835113,1.85685975]	5, 65
$-\infty$	[-0.23945,-0.23918]	[1.85713483,1.86457648]	66
$10, -\infty$	[-0.23917,-0.23915]	[1.86485263,1.86512882]	34, 66
$20, -\infty$	-0.23914	1.86568132	40, 60
$-\infty$	[-0.23913,-0.23643]	[1.86595763,1.94198797]	66
$7, 14, 28, -\infty$	[-0.23642,-0.23640]	[1.94227494,1.94284899]	32, 68
$-\infty$	[-0.23639,-0.23349]	[1.94313608,2.02812202]	67

TABLE I

ATTRACTORS, INTERVALS AND RELATIVE SIZE OF BASINS OF ATTRACTION.

$(1,3)$	$\longleftrightarrow$	$(41.39\%, 4.93\%)$	$(2,6)$	$\longleftrightarrow$	$(43.25\%, 6.19\%)$
$(4,12)$	$\longleftrightarrow$	$(35.86\%, 6.60\%)$	$(8,24)$	$\longleftrightarrow$	$(35.00\%, 6.67\%)$
$(16,48)$	$\longleftrightarrow$	$(34.83\%, 6.63\%)$	$(32,96)$	$\longleftrightarrow$	$(34.66\%, 6.65\%)$
$(64,192)$	$\longleftrightarrow$	$(34.70\%, 6.65\%)$			

TABLE II

RELATIVE BASIN SIZES WHEN TWO MEMBERS OF THE 1×2^i AND 3×2^j CASCADES COEXIST.

$(1,9)$	$\longleftrightarrow$	$(41.39\%, ****)$	$(1,15)$	$\longleftrightarrow$	$(41.39\%, 7.16\%)$
$(2,18)$	$\longleftrightarrow$	$(43.25\%, 6.57\%)$	$(2,30)$	$\longleftrightarrow$	$(43.25\%, 7.16\%)$
$(4,36)$	$\longleftrightarrow$	$(35.86\%, 6.66\%)$	$(4,60)$	$\longleftrightarrow$	$(35.86\%, 7.16\%)$
$(8,72)$	$\longleftrightarrow$	$(35.00\%, 6.65\%)$	$(8,120)$	$\longleftrightarrow$	$(35.00\%, 7.16\%)$
$(16,144)$	$\longleftrightarrow$	$(34.83\%, 6.65\%)$	$(16,140)$	$\longleftrightarrow$	$(34.83\%, 7.16\%)$

TABLE III

RELATIVE BASIN SIZES WHEN TWO MEMBERS OF THE 1×2^i AND 18×2^j CASCADES COEXIST.